



Heat transfer efficient thermal energy storage for steam generation

R. Adinberg*, D. Zvegilsky, M. Epstein

Solar Research Facilities, Weizmann Institute of Science, Rehovot 76100, Israel

ARTICLE INFO

Article history:

Received 14 April 2008

Received in revised form 7 January 2009

Accepted 12 August 2009

Available online 25 September 2009

Keywords:

Thermal storage

Zinc alloy

Reflux

Heat transfer

Solar power

Steam

ABSTRACT

A novel reflux heat transfer storage (RHTS) concept for producing high-temperature superheated steam in the temperature range 350–400 °C was developed and tested. The thermal storage medium is a metallic substance, Zinc–Tin alloy, which serves as the phase change material (PCM). A high-temperature heat transfer fluid (HTF) is added to the storage medium in order to enhance heat exchange within the storage system, which comprises PCM units and the associated heat exchangers serving for charging and discharging the storage. The applied heat transfer mechanism is based on the HTF reflux created by a combined evaporation–condensation process. It was shown that a PCM with a fraction of 70 wt.% Zn in the alloy (Zn70Sn30) is optimal to attain a storage temperature of 370 °C, provided the heat source such as solar-produced steam or solar-heated synthetic oil has a temperature of about 400 °C (typical for the parabolic troughs technology). This PCM melts gradually between temperatures 200 and 370 °C preserving the latent heat of fusion, mainly of the Zn-component, that later, at the stage of heat discharge, will be available for producing steam. The thermal storage concept was experimentally studied using a lab scale apparatus that enabled investigating of storage materials (the PCM–HTF system) simultaneously with carrying out thermal performance measurements and observing heat transfer effects occurring in the system. The tests produced satisfactory results in terms of thermal stability and compatibility of the utilized storage materials, alloy Zn70Sn30 and the eutectic mixture of biphenyl and diphenyl oxide, up to a working temperature of 400 °C. Optional schemes for integrating the developed thermal storage into a solar thermal electric plant are discussed and evaluated considering a pilot scale solar plant with thermal power output of 12 MW. The storage should enable uninterrupted operation of solar thermal electric systems during additional hours daily when normal solar radiation is not sufficient.

© 2009 Elsevier Ltd. All rights reserved.

1. Introduction

High-temperature superheated steam generated in concentrated solar power plants is an environmentally clean energy carrier that can be efficiently utilized for electricity production via the conventional Rankine cycle. The major solar radiation concentrating technologies being developed for steam production are the parabolic trough, linear Fresnel trough, power tower and parabolic dish [1,2].

In consideration of solar irradiation as an essentially intermittent source of energy, all those solar power technologies need to be integrated with adequate thermal storage capacities in order to: (a) provide stable steam generation while the radiant energy is unsteady and (b) extend the system operation for additional hours daily when the sun is not available. By means of thermal storage the annual capacity factor of a solar power plant can be doubly increased achieving 50% or more [2], which leads to a better system performance and reduced electricity cost.

Energy storage materials considered in the literature for solar steam power systems in the temperature range from 200 to 600 °C are mainly inorganic salts (pure substances and eutectic mixtures), e.g. NaNO₂, NaNO₃, KNO₃, etc. [3–5]. The process of thermal storage using molten salts as the heat transfer and storage medium is based on either a temperature change occurring in the storage system – the sensible heat mode or the phase transition upon melting/solidification – the latent heat mode [4].

Presently, the sensible heat mode is a well advanced and practically demonstrated storage technology being developed into two basic options [2,4]: a two-tank and thermocline systems. The biggest challenges faced by this technology are a relatively high freezing point of the candidate molten salts (e.g. 220 °C for a binary mixture of 60% NaNO₃ and 40% KNO₃, known as the solar salt), up-scaling to a large commercial size with several hours of energy storage and considerable reduction of capital costs for the storage systems.

Latent heat storage systems have the potential advantages of storing a larger amount of energy per unit mass, as compared to the sensible heat mode, and producing steam under isothermal conditions, near the temperature of salt fusion, with a constant

* Corresponding author. Tel.: +972 8934 3779; fax: +972 8934 4117.
E-mail address: roman.adinberg@weizmann.ac.il (R. Adinberg).

power throughput. However, using of molten salts as phase-change materials (PCM) impose great difficulties on the storage structure design, which typically comprises heat exchangers for heat input and output embedded in the storage medium.

A major problem of latent heat storage is solidification of PCM on the surface of the heat exchanger during heat discharge [6,7]. Solid salt deposits cause significant resistance to heat transfer in both the charge and discharge processes. In addition there are severe corrosion and mechanical issues concerning the storage construction materials that can significantly increase the cost of energy storage.

A number of solutions improving the heat transfer from PCM to steam have been investigated, including encapsulation of storage material, application of intermediate heat transfer fluid and using of composite materials based on a highly conductive natural graphite and PCM [5,7,8]. Several metal PCM materials such as Li, Sn, Zn and eutectic alloys have also been evaluated [3,9,10] and the obtained results demonstrate a significantly better thermal performance for metals than for molten salts under the same volume.

In the present research work a reversible cycle of thermal energy input and output making use of a metal alloy PCM in combination with a highly enhanced heat transfer pattern was investigated. This novel latent heat storage concept is primarily suitable for parabolic trough solar collectors where the steam temperature can reach about 400 °C.

2. Reflux heat transfer storage (RHTS) concept

The RHTS concept is based on a synergistic utilization of phase change effects of melting and vaporization occurring in the thermal energy storage medium. For this reason, a low melting point substance, for instance liquid metal or synthetic organic oil, is added to the PCM, to deliver thermal energy between the storage medium and externally located heat exchangers by reflux of the heat transfer fluid (HTF) via evaporation and condensation. This heat transfer pattern is similar to one effectively working in thermosyphons and pool-boilers. It is important that the storage vessel be thoroughly evacuated of water vapors and other gases in the beginning and kept continually leak-tight for both vacuum and pressure conditions.

Choosing the HTF involves several prerequisites including high-temperature stability, chemical compatibility and minor mutual solubility with the PCM, non-corrosiveness to the structural materials, low density in comparison with the PCM, and a sufficient vapor pressure at the operating temperature. Feasibility of this storage concept was first successfully demonstrated using a PCM-HTF system composed respectively of sodium chloride salt and sodium metal for a storage temperature of 800 °C [11].

Fig. 1 illustrates the schematic of RHTS storage intended to produce high-temperature steam when the solar steam generation process is temporarily interrupted. HTF is used to transfer heat between the thermal storage medium – PCM and two heat exchangers (HE) placed externally of the PCM at the bottom and the top and of the storage vessel. The top HE, i.e. steam generator, is fed with high pressure water (return condensate) to produce superheated steam during the storage discharge cycle. The bottom HE is used to charge the thermal storage. It is immersed in the liquid HTF and connected to the solar working fluid, e.g. a flow of solar superheated steam or solar-heated synthetic oil. During heat charge cycles, due to pool-boiling of the HTF, there is an intensive flow of vapors up through the transport channels distributed in the PCM. By condensation on the channels' surfaces and directly on the surface of the PCM, the latent energy of vapors is transferred across the walls to the PCM. On discharge, the heat flow direction is re-

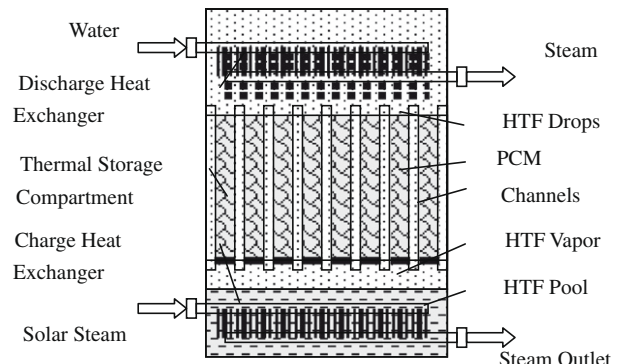


Fig. 1. Schematic diagram of the RHTS concept.

versed. The hot PCM causes the liquid HTF to evaporate and the vapors transmit heat to the top located steam generator via the mechanism of condensation.

From a preliminary study on the selection and characterization of thermal storage materials, the following PCM-HTF pair appeared to be suitable for the target temperature of 400 °C:

- **PCM:** Zinc-Tin alloy containing 70 wt.% Zn (Zn70Sn30). This substance has a liquidus temperature of 370 °C that requires a heat carrier to charge the storage, such as the solar superheated steam, with a temperature close to 400 °C. On discharge the release of heat is due mainly to the latent heat of zinc solidification and partly to sensible heat of the alloy liquid phase, while the storage temperature decreases gradually toward the eutectic point at 198.5 °C [12].
- **HTF:** Eutectic mixture of 26.5% biphenyl and 73.5% diphenyl oxide which is produced commercially as a high-temperature (up to 400 °C) thermal fluid. Equilibrium vapor pressure of this HTF is about 11 bars at the maximum storage temperature [13].

3. Storage materials testing

The storage medium comprising the alloy Zn70Sn30 and HTF has been examined for compatibility and thermal stability of the components under temperature conditions typical for the thermal process of steam generation. Alloy Zn70Sn30 was specifically manufactured using the base metals of technical-purity grade by Numinor Chemical Industries Ltd. (Israel). The major impurity determined in the product was iron which was the material of the crucible employed in the alloy production. The HTF was purchased as a commercial product Dowtherm-A produced by Dow Chemical Co. Specimens of the PCM and HTF chemicals were subjected, separately and jointly, to a sequence of laboratory testing procedures which included maintaining a constant substances temperature 400 °C and varying the temperature between 200 and 400 °C.

3.1. Ampoule tests

This test procedure consisted of the following steps:

- Preparing hermetically sealed glass ampoules (10 ml capacity) filled with a few grams of Zn70Sn30 alloy (particles of a size 2–3 mm) along with a few milliliters of the liquid HTF. In some of the ampoules, stainless steel (316L) pieces were added to test the effect of a potential storage structure material.
- Placing the ampoules into a laboratory high-temperature oven and holding them at 400 °C at least 8 h. The heating routine was repeated 3–4 times at regular intervals with each ampoule.

- Post-test visual inspection of the ampoules at ambient temperature for: integrity (some might burst), change of color, physical state, additional phases, etc.
- Examining the content of ampoules by means of Differential Thermal Analysis (TA Instruments TG/DTA Q600 system) and FTIR Spectroscopy (Brukner FTIR Analyzer TENSOR 27).

It is shown in Fig. 2 that some visible changes could be typically observed after the first heating of a test ampoule:

1. The solid particles became fully fused as a result of heating above the liquidus point, 370 °C.
2. The liquid, first transparent and colorless, appeared to be yellowish-red. This is likely an effect of opalescence caused by reaction of the liquid with air remaining in the ampoule after sealing. The same change in color occurred when the HTF was sealed in ampoules and heated above 200 °C with no presence of supplemental materials. This change of color (no difference in the FTIR spectrum could be detected) has no consequences on the performance of the thermal storage.
3. No further visible modifications of the ampoule contents were discovered after repeating the heating procedure several times.

About 20 ampoules containing PCM–HTF–Steel samples were tested accordingly. All of them, without exception, showed satisfactory results in terms of thermal stability and compatibility of the storage materials. In addition, the remarkable thermal stability of the selected PCM–HTF system was verified under continuous 30-days heating of the test ampoules at 400 °C.

3.2. Heat cycling tests

Fig. 3 represents a diagram of the lab calorimetric set-up used for testing the storage materials under thermal conditions typical of a full scale system. A temperature controlled furnace is used to heat the sampler vessel containing alloy Zn70Sn30 (1500 g) and Dowtherm-A (450 ml) to a temperature of 380 °C. As shown in the diagram, the sampler vessel together with vertical tubes (1) and (2) and coil (3) form a closed loop for HTF flow. A valve installed on the tube (2) is used to block the fluid flow while heating of the sample is activated.

After melting the sample and reaching the required temperature, the oven is switched off and the valve is opened to allow HTF to flow and circulate. During that period the heat of the PCM sample is transferred to the water condenser by HTF due to the subsequent processes of liquid evaporation taking place in the sampler vessel, rising of the vapors in the tube (1) and vapor con-

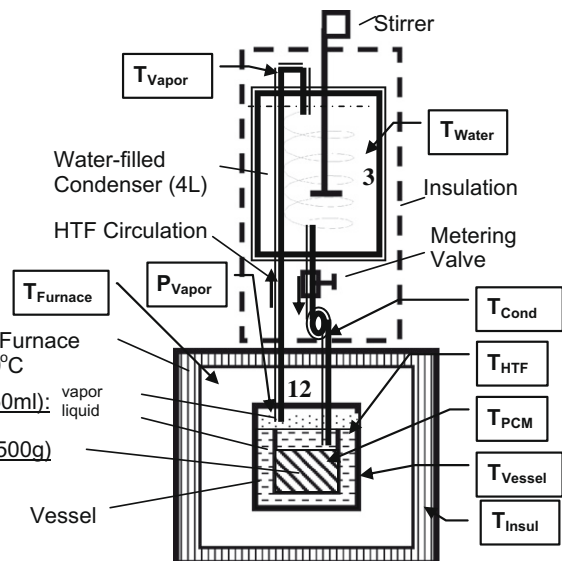


Fig. 3. Schematic representation of the lab calorimetric set-up. Points of measurements: T -temperature, P -pressure.

ensation occurring in the coil. Gravity is utilized to return the HTF condensate through the tube (2) back to the sampler vessel.

The points of measurements, which included temperature in different location of the system and HTF vapor pressure, are shown in Fig. 3 and specified in Table 1.

On the heat discharge, typical temperature ranges were approximately 380–200 °C for the sample and 25–50 °C for the water accompanied with HTF pressure drop from 8.5 to 0.2 bar. Multiple cycles with different rates of heat charge and discharge were made possible by controlling the oven and metering valve correspondingly. After each cycle the hot water was replaced with the same quantity of cold (room temperature) water – 3.8 l. According to the energy balance, the heat supplied to the water equates the decrease of enthalpy of the sample, taking into account the calibrated heat losses.

This experimental apparatus enabled investigating materials compatibility and simultaneously studying thermal effects developed during the heat charge and discharge cycles in the storage system. The method of testing the storage materials was based on monitoring the temperature and pressure of HTF continuously, as illustrated in Fig. 4.

In the case of proper operation, the vapor pressure of HTF should follow closely the thermodynamic equilibrium data available for this fluid [13]. If the thermal fluid fails due to thermal decomposition or reacting with PCM or other materials in direct contact, a significant deviation of pressure from the equilibrium value at the operating temperature could be expected. In total, more than 100 thermal cycles with the same load of storage materials were performed. Similar to the run depicted in Fig. 5, all the other experimental results exhibited without exception excellent thermal stability of the Zn70Sn30 – Dowtherm-A storage materials system under the corresponding variations of temperature between 200 and 380 °C.

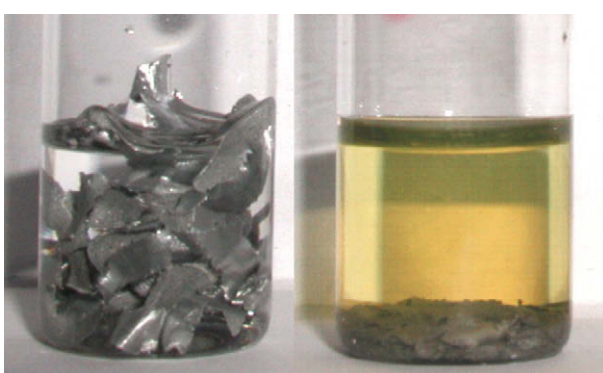


Fig. 2. A test ampoule before (left) and after (right) heating at 400 °C for 8 h. The ampoule was initially loaded with Zn70Sn30 particles and HTF, the colorless liquid.

4. PCM calorimetry

Fig. 6 shows an equilibrium phase diagram of the Zn–Sn alloy having a eutectic point at a temperature of 198.5 °C and a Zn fraction nearly 9 wt.%. Main physical states of the system are: above the liquidus – entirely liquid mixture, below the eutectic temperature – entirely solidified alloy, and the middle part is composed of

Table 1

Points of measurements applied in the heat cycling tests as shown in Fig. 3.

Parameter and Maximal Experimental Value	Notation	No. of Points	Sensor	Accuracy
PCM temperature inside the sampler vessel, 380°C	T _{PCM}	2	Thermocouple type K	1.5°C
HTF temperature inside the sampler vessel, 380°C	T _{HTF}	2		
HTF vapor temperature in tube (1), 380°C	T _{Vapor}	1		
HTF condensate temperature in tube (2), 80°C	T _{Cond}	1		
Furnace temperature, 420°C	T _{Furnace}	3		
Water bulk temperature, 50°C	T _{Water}	6	Thermocouple type T	0.5°C
HTF vapor pressure in the sampler vessel, 8.5 bar	P _{Vapor}	1	Pressure transducer	0.05 bar

liquid tin and partly liquid, partly solid zinc at the same temperature. The relevant heat storage region is left of the eutectic point and below the liquidus.

In Fig. 6, point A represents the composition of Zn70Sn30 in an equilibrium state at the liquidus temperature of 370 °C. As soon as cooling is applied, this molten alloy starts to form solid zinc. When the temperature drops continually, the amount of zinc solidified gradually increases and the composition of remaining liquid becomes proportionally richer in tin. As a result, the temperature needed to freeze the remaining zinc becomes lower. At the eutectic point, about 81 wt.% of the Zn is solidified. Upon heating, the system can be reversed back into the initial molten state. To calculate the system calorific properties, a simple mixture relation was assumed, i.e. arithmetic average, using fusion enthalpies and specific heat coefficients of liquid and solid Zn and Sn taken from [14]. With the temperature decrease of 100 °C between points A and B (Fig. 6), the total enthalpy change of the PCM equals 107 kJ/kg, which is composed of the sensible heat of liquid –37 kJ/kg and the released heat of fusion of zinc –70 kJ/kg. Obviously, the zinc phase change is a dominating factor in this process. The more zinc in the composition and the greater the temperature difference, the higher energy storage capacity is attained. A PCM composition of 100% zinc could be most favorable for the heat storage, since the heat of fusion for pure zinc is $\Delta H_f = 112 \text{ kJ/kg}$ and the same temperature is obtained for both the charge and discharge. However, the melting point of zinc is 420 °C, which is beyond the maximum working temperature of the HTF employed (400 °C). Presently, the heat carrier used to charge thermal storage is supposed to have a

temperature of 400 °C. This limits the zinc percentage in the alloy to no more than 70 wt% in order to have a sufficient temperature gradient of at least 30 °C between the solar heat carrier and PCM.

The heat of fusion for Zn is rather low based on a unit of mass and compared to that of typical salt-based storage materials, e.g. NaNO₃ (melting point 307 °C, $\Delta H_f = 172 \text{ kJ/kg}$, solid density 2.26 g/cm³). However, taking into account the high density of zinc (7.14 g/cm³) its fusion heat per unit of volume is about twice that of the molten salts. Hence, the metallic PCM offers a more compact and cost effective thermal storage design.

5. Solar power plant layout

Heat storage capacity along the A–B line (see Fig. 6) can be increased mainly on account of a reduced temperature B. Then from the beginning to the end of the process the temperature of steam produced on discharge would drop approximately by the same temperature range, equal or larger than 100 °C. However, steam temperature variations of over 20 °C can significantly reduce the steam turbine efficiency.

In order to narrow the range of steam temperature from a non-isothermal storage, a method depicted in Fig. 7, is proposed. In this arrangement the thermal storage system is assembled of two RHTS-based components: the main energy storage unit and a thermal buffer. The buffer is set to level the time-variable temperature of steam after the main storage. With the same PCM filled in both units the buffer capacity, as it is shown farther, can be much smaller relative to the main storage. Functioning of a buffer is explained

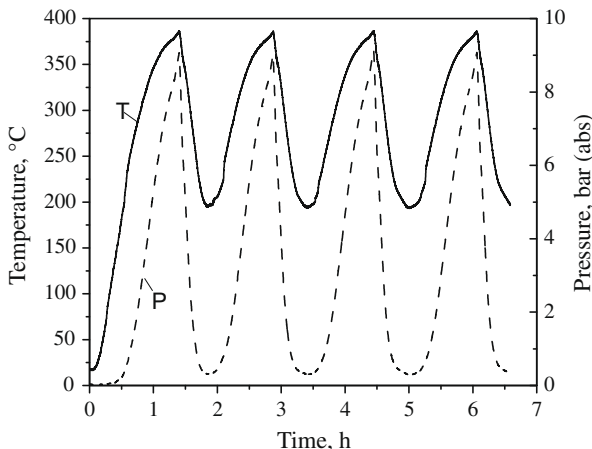


Fig. 4. Typical PCM temperature (T) and HTF pressure (P) experimental data measured inside the sampler vessel of the lab calorimetric set-up.

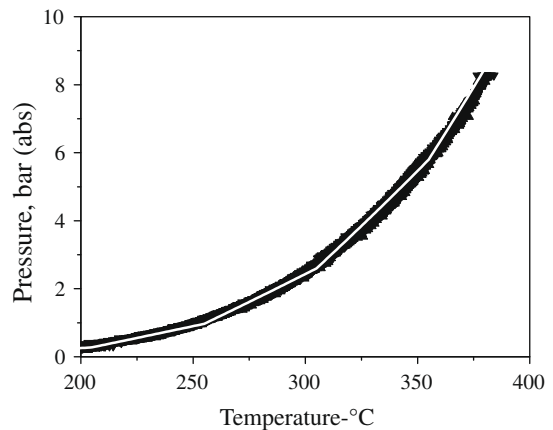


Fig. 5. HTF vapor pressure vs. temperature: white curve – equilibrium data for Dowtherm-A [13], black strip – experimental points obtained from one thermal cycle of sample heating and cooling.

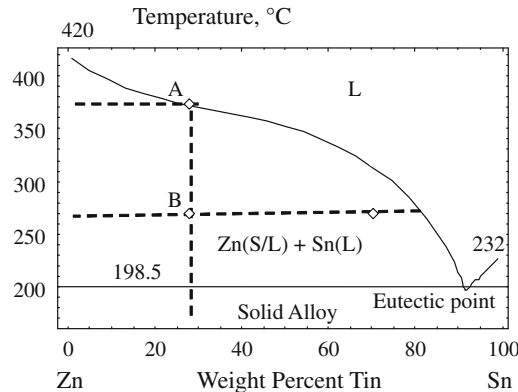


Fig. 6. Zn–Sn phase diagram based on thermodynamic data [12].

as: (a) at the beginning of the charge phase the buffer must be at a higher temperature than the main storage to be able to partly compensate the significant drop of steam temperature occurring in the main storage, (b) later, during the charge, as the main storage temperature is increased, the steam temperature might gradually become higher than that of the buffer. Then part of the steam energy is transferred to the buffer, recovering its temperature, and (c) the process is reversed on the discharge, working to retain the steam temperature at a given level.

According to the process scheme shown in Fig. 7, solar superheated steam produced during sunlight hours, for instance at pressure 70 bar (water boiling point 287 °C) and temperature 400 °C, is supposed to charge the thermal storage system and subsequently to feed the steam turbine. Even though, after the thermal storage system, the quality of the solar superheated steam is reduced by e.g., 50 °C, it can still efficiently operate steam turbines. When solar energy, partly or absolutely, is not available, the thermal storage might be capable of retaining the same steam mass flow without temporarily losing the operational continuity, for a period dependent on the storage capacity. Note that for this “serial” connection of thermal storage to a solar power system, the storage variables such as thermal capacity and charge and discharge periods of time cannot be fixed independently for they are strictly dependent on the operation parameters (mainly the mass flow rate) of the solar steam used to charge the storage system.

Alternatively, a thermal storage system can be detached from the main stream of solar steam and provided with a supplemental solar power facility allocated for charging the storage. An important characteristic of the parallel-connected storage shown in

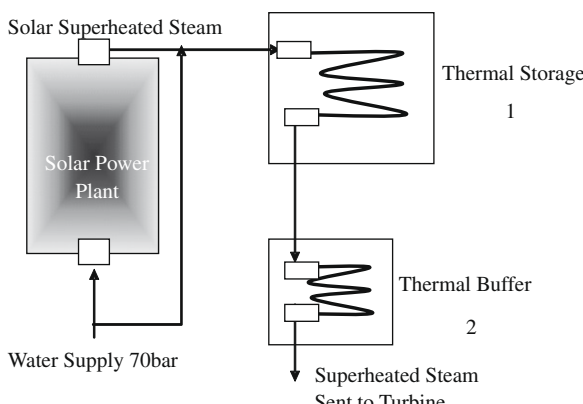


Fig. 7. Two-stage RHTS system integrated into a solar power plant using the serial connection mode: solar superheated steam charges the thermal storage system and feeds a steam turbine, successively.

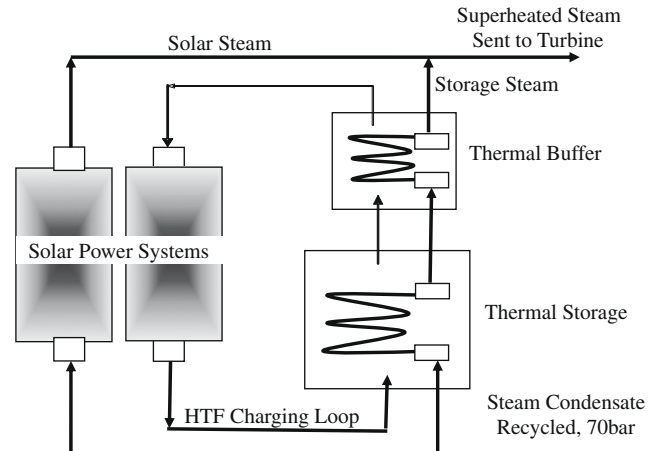


Fig. 8. The parallel-connected two-stage RHTS system.

Fig. 8 is its ability to adapt arbitrary large thermal capacities by coupling a proper solar power supply. In addition, the storage designated solar system has the advantage of employing as same heat carrier as the HTF used in the RHTS unit.

6. Pilot RHTS storage evaluation

RHTS performance parameters of a pilot scale solar thermal energy storage system were calculated using heat balance equations written in similar way for both the main storage and the buffer unit:

$$q_S = m_S \frac{dE_{PCM}[T[t]]}{dt} \quad (1)$$

$$q_F = M_F(E_F[T_2[t]] - E_F[T_1[t]]) \quad (2)$$

$$q_{HE} = kA\Delta T[t] \quad (3)$$

$$q_F = q_S = q_{HE} \quad (4)$$

In the set of equations above, Eq. (1) describes the change of PCM enthalpy E_{PCM} (quantity m_S , bulk temperature T) in time t , Eq. (2) – enthalpy change of fluid (water/steam or HTF with a mass flow rate M_F) between outlet and inlet, including water–steam phase transition, Eq. (3) – heat transfer in the heat exchanger determined by the convective heat transfer coefficient k , surface area A , and log mean temperature difference between PCM and fluid ΔT , and Eq. (4) – overall balance of heat in the system at any time t .

The two basic options of thermal storage installation, regarding the serial and parallel connections introduced above, were evaluated for a solar power plant producing superheated steam at a nominal rate of 28 ton/h, equivalent to 12–13 MW thermal power output at a steam temperature close to 350 °C.

Table 2 gives input values used in the pilot RHTS calculations. The period of charge was set to 6 h, taking this value as the duration of an annual average operational day with nominal solar power supply. Concerning the period of discharge, this variable is treated differently in relation to the serial and parallel connections. In the first case, the period of discharge has to be found from the numerical solution using a storage capacity value which is actually fixed in advance through the input parameters of solar steam flow and duration of charge. In the second case, it can be given as a requirement, for instance 4 h as in **Table 2**, and then the storage capacity is obtained from the solution. An additional condition was attached to Eqs. (1)–(4) considering steam flow within the two-stage RHTS system: temperatures at the main storage outlet and buffer inlet are equal all the time during storage operation.

Table 2

Data applied in the RHTS simulations for serial and parallel storage connections; both required a thermal power nominal output of 12 MW.

Parameter	Units	Serial	Parallel
Storage steam mass flow rate	ton/h	28	
Water input temperature	°C	250	
Water boiling point (70 bar)	°C	287	
Solar steam temperature	°C	400	-
Solar steam mass flow rate	ton/h	28	-
HTF solar loop temperature	°C	-	400
HTF solar loop mass flow rate	ton/h	-	346
Storage temperature at beginning of charge	°C	290	
Storage temperature at end of charge	°C	370	
Buffer temperature at beginning of charge	°C	360	
Charge period	h	6	
Discharge period	h	not assigned	4

To facilitate the present evaluations there were no specific RHTS designs introduced into the simulation problem. The complicated models for different heat transfer patterns that might occur in the storage system structure were replaced with estimates for the heat transfer coefficient k available in literature [15,16], particularly dealing with such phenomena as boiling, condensation and convection. Following this approach, the numerical parameter A (surface area) used in Eq. (3) was adjustable to obtain a small temperature difference ΔT of about 10–20 °C. For the same reason, neither heat loss nor pressure drops were presently taken into account.

Numerical solutions of the system of Eqs. (1)–(4) were obtained using the Mathematica 6.0 software [17]. The results of simulations are summarized in Table 3 along with Figs. 9 and 10 showing temperature transitions for different components of the serial- and parallel-connected RHTS systems during a complete charge–discharge cycle. With the charge period of 6 h and other input parameters defined in Table 2, the serial storage solution yields a capacity equal to 4 MW h for fully charged thermal storage. This is a rather low value that provides the nominal output of superheated steam during

Table 3
Simulation results for the prime RHTS parameters.

Parameter	Units	Serial	Parallel
Main storage PCM mass	ton	150	2000
Buffer PCM mass	ton	60	600
Storage capacity	MW h	4	52
Discharge period	h	0.3	(4)

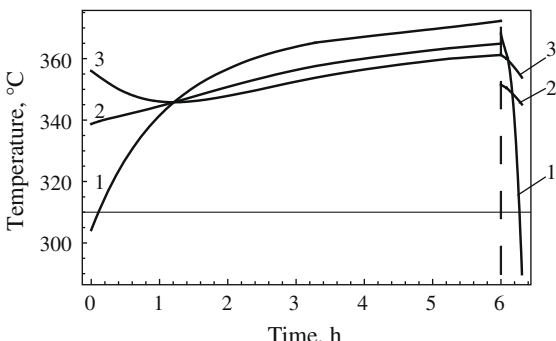


Fig. 9. Temperature variations calculated for the serial-connected RHTS unit. Thermal storage capacity: 4 MW h. Cycle periods: 6 h for charge and 20 min for discharge. Notations: 1 – steam exiting the main storage, 2 – steam exiting the buffer, 3 – buffer PCM.

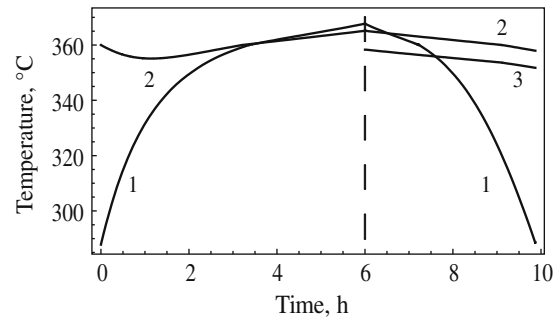


Fig. 10. Temperature variations calculated for the parallel-connected RHTS unit. Thermal storage capacity: 52 MW h. Cycle periods: 6 h for charge and 4 h for discharge. Notations: 1 – main storage PCM, 2 – buffer PCM, 3 – storage superheated steam outlet.

20 min only. As was already commented above, the restriction is due to the fixed parameters of solar steam used to charge thermal storage in the serial connection scheme. Obviously such a system is not applicable for relatively large storage capacities to be operated for heat discharge on a time scale of hours. In that case the period of charge must be, for instance, as long as several days in order to attain the storage-based steam production during 2–3 h.

From Table 3, the arbitrary chosen period of discharge 4 h is available with the parallel-connected RHTS system which contains an amount of PCM (Zn70Sn30 alloy) equal to 2600 tons in total. To be fully charged up to a thermal capacity of 50 MW h, this storage system requires a solar parabolic trough system supplying heat by means of a high-temperature (400 °C) HTF flow with a mass rate of 346 ton/h during 6 h. Optionally, any combinations of heat charge and discharge periods can be accomplished with the parallel-connected storage for a requested steam output. Finding a proper match should include careful consideration concerning the technical feasibility of a specific storage system design accompanied with economic efficiency of the entire assembly of a solar thermal electric plant.

It is also important to note that the two-stage configuration of RHTS storage is highly efficient in equalizing the steam output temperature in time for both the serial and parallel connections. From Fig. 9, the comparison of curves 1 (main storage outlet) and 2 (buffer outlet) shows that setting a buffer unit after the main storage changes the overall steam temperature difference from about 80 °C to a maximum 20 °C. During the full operational cycle, comprised of charge and discharge periods, steam sent to the turbine has a reasonably stable temperature 340–360 °C (Fig. 9, curve

2). Fig. 10 illustrates similar uniformity of steam temperature (curve 3) obtained throughout a long discharge period of 4 h.

7. Summary and conclusions

The experimental results of this work have shown that a novel latent heat materials system composed of the commercially available products: alloy-Zn70Sn30 as PCM and eutectic mixture of biphenyl/diphenyl oxide as HTF possesses the proper thermo-physical properties, chemical compatibility and thermal stability required for the thermal storage to operate a superheated steam generator at a temperature of near 350 °C. This chemical compound laid a basis for developing the RHTS storage concept that integrates the PCM solid-liquid and HTF liquid-vapor reversible phase change processes, both running simultaneously for respectively storing and transferring heat in the thermal storage system.

Aimed at extending the operating time of solar thermal electric systems during periods of reduced solar radiation, the thermal storage system has been assembled from two RHTS-based components: the main energy storage unit and a thermal buffer, arranged in series. The buffer is necessary to settle the time-variable temperature of steam after the main storage. The primary reason for the steam temperature variation is that the storage PCM composition of 70% zinc (balance tin) is far from the eutectic point (9% Zn). Therefore, the alloy solidifies gradually when the temperature decreases from 370 to 200 °C causing the thermal process to be intrinsically non-isothermal. According to heat balance computations performed using the same PCM-HTF material system in both storage units, the buffer allows to maintain the steam outlet temperature within a narrow range of 340–360 °C during all the storage operation. This result is achieved by the specific synchronization of main storage and buffer during charge and discharge operations. In general, heat storage capacity needed to be allocated for a buffer is much smaller (2–3 times) than that of the main storage unit.

The basic options of integrating RTHS storage into solar power plants, the serial connection – utilizing the prime solar system, and the parallel connection – utilizing a supplementary solar system, have been evaluated assuming a pilot scale solar power plant of 12 MW thermal power output (superheated steam temperature 350 °C and pressure 70 bars). It is shown on the basis of 6 h charge duration that the serial-connected storage might have a rather limited thermal capacity adequate for only a 20 min period of nominal steam throughput. Compared to this simple and relatively inexpensive integration concept, the parallel connection scheme would require a substantial investment in the extra solar power installation which, however, is rewarded by theoretically unlimited thermal capacity, as in the given example of 4 h storage discharge capability.

The development of the RHTS concept has been focused mainly on resolving the heat transfer problems associated with molten salts commonly utilized as PCM in conventional thermal storage systems. Although the proposed Zn70Sn30 PCM will most certainly

be more expensive than any of these salts, RHTS applications can probably be rewarding as the end result of a significantly improved thermal storage performance based on the following factors:

- Outstanding chemical stability of the tested Zn70Sn30 – HTF system.
- High substance density and superior thermal conductivity of Zn70Sn30, roughly 50 W/m-K in liquid state that is about two orders of magnitude over molten salts.
- High heat transfer quality demonstrated in the experiments that can be compared to the utility of thermosyphons.

Acknowledgment

This work was supported by the EU 6th International Framework Program under Contract No. SES6-CT-2004-503526.

References

- [1] Müller-Steinhagen H, Trieb F. Concentrating solar power: a review of the technology. *Ingenia*, Roy Acad Eng 2004(18):43–50.
- [2] An assessment of solar energy conversion technologies and research opportunities. GCEP energy assessment analysis – Summer 2006. Issued by the Global Climate and Energy Project, Stanford University. <http://gcep.stanford.edu/pdfs/assessments/solar_assessment.pdf> [accessed 03.12.08].
- [3] Hoshi A, Mills DR, Bittar A, Saitoh TS. Screening of high melting point phase change materials (PCM) in solar concentrating technology based on CLFR. *Sol Energy* 2005;79(3):332–9.
- [4] Herrmann U, Kearney DW. Survey of thermal energy storage for parabolic trough power plants. *Transactions of the ASME*. *J Sol Energy Eng* 2002;124:145–52.
- [5] Zalba B, Marin JM, Cabeza LF, Mehling H. Review on thermal energy storage with phase change, Heat transfer analysis and applications. *Appl Therm Eng* 2003;23:251–83.
- [6] Application of solar technology to today's energy needs – vol. 1, ch. XI energy storage; June 1978. NTIS order #PB-283770. <http://www.princeton.edu/~ota/ns20/year_f.html> [accessed 03.12.08].
- [7] Steinmann W-D, Eck M, Laing D. Solarthermal parabolic trough power plants with integrated storage capacity. *Int J Energy Technol Policy* 2005;3(1/2):123–36.
- [8] Haillot D, Py X, Goetz V, Benabdellah M. Storage composites for the optimisation of solar water heating systems. *Chem Eng Res Des* 2008;86:612–7.
- [9] Chow LC, Zhong JK. Thermal conductivity enhancement for phase change storage media. *Int Commun Heat Mass Transfer* 1996;23(1):91–100.
- [10] Birchenall CR, Riechman AF. Heat storage in eutectic alloys. *Metall Trans A* 1980;11A:1415–20.
- [11] Adinberg R, Yogeve A, Kaftori D. High temperature thermal energy storage. *J Phys IV France* 1999;9:89–94.
- [12] Mozer Z, Dutkiewicz J, Gasior W, Salawa J. The Sn-Zn (Tin-Zinc) System. *Bull Alloy Phase Diagrams* 1985;6(4):330–4.
- [13] DOWTHERM A technical data sheet. <<http://www.dow.com/heattrans/tech/data.htm>> [accessed 14.12.08].
- [14] Outokumpu HSC chemistry for windows. Chemical reaction and equilibrium software with extensive thermochemical database, version 5. <<http://www.outokumpu.com/hsc>> [accessed 14.12.08].
- [15] Collier J, Thome JR. Convective boiling and condensation. 3rd ed. Oxford Science Publication; 2001.
- [16] Grigull U, Sandner H. Heat conduction. Hemisphere Publishing Corporation; 1984.
- [17] Wolfram Research, Inc. <<http://www.wolfram.com>> [accessed 14.12.08].